Brief Papers

Voltage-Controlled Oscillators up to 98 GHz in SiGe Bipolar Technology

Werner Perndl, Herbert Knapp, Klaus Aufinger, Thomas F. Meister, Werner Simbürger, and Arpad L. Scholtz

***Abstract*—In this paper, two fully integrated voltage-controlled oscillators (VCOs) in a 200-GHz f_T SiGe bipolar technology are presented. The oscillators use on-chip transmission lines at the output for impedance transformation. One oscillator operates up to 98 GHz and achieves a phase noise of −85 dBc/Hz at an offset frequency of 1 MHz. It can be tuned from 95.2 to 98.4 GHz and it consumes 12 mA from a single −5-V supply. The second oscillator operates from 80.5 GHz up to 84.8 GHz with a phase noise of −87 dBc/Hz at 1-MHz offset frequency. The output power of both circuits is about −6 dBm.**

***Index Terms*—Phase noise, phase noise measurement, SiGe, voltage-controlled oscillator (VCO), waveguide.**

I. Introduction

VOLTAGE-CONTROLLED oscillators (VCOs) are key components in many applications ranging from communication systems to radar distance sensors. Since the demand on bandwidth increases continuously, circuits for higher frequency bands are required. The highest frequency fundamental-mode oscillator reported so far operates up to 146 GHz and is fabricated in an InGaP–InGaAs technology with an $f_{\max}$ of 170 GHz [1]. In silicon-based technologies, VCOs with operation frequencies up to 60 GHz [2], 88 GHz [3], and recently, 100 GHz [4] have been reached so far. An oscillator design up to 50 GHz which exhibits a very low phase noise of −110 dBc/Hz at an offset frequency of 1 MHz has been presented in [5].

In this paper, two fundamental-mode VCOs with different resonator designs are presented. The main attention was given to reach very high oscillation frequencies without neglecting phase noise and output power. The circuit concept is based on the Colpitts oscillator. It includes a quarter-wave transformer at the output for impedance transformation, which is a novelty for silicon-based technologies.

The results of the VCOs have been recently presented by the authors [6]. In this paper, circuit design and technology parameters are presented in more detail. Additionally, the influence of the measurement equipment on the results are discussed which affected phase noise data in [6].

Manuscript received December 11, 2003; revised May 14, 2004.

W. Perndl is with Infineon Technologies AG, D-81739 Munich, Germany, and also with the University of Technology Vienna, 1040 Vienna, Austria (e-mail: werner.perndl@infineon.com).

H. Knapp, M. Wurzer, K. Aufinger, and W. Simbürger are with Infineon Technologies AG, D-81739 Munich, Germany.

A. L. Scholtz is with the University of Technology Vienna, 1040 Vienna, Austria.

Digital Object Identifier 10.1109/JSSC.2004.833757

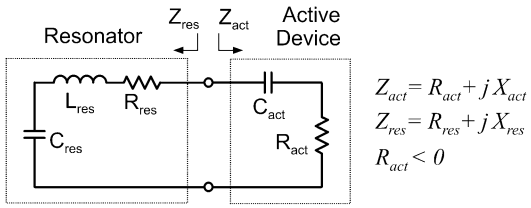

Fig. 1. Negative impedance model for analyzing oscillators.

II. Circuit Design

A. Oscillator Model

Oscillators can be analyzed either as amplifiers with positive feedback or as negative impedance circuits. At the beginning of the design process, we analyze the oscillators with the negative impedance model shown in Fig. 1. This model consists of an active device represented by a negative resistance with a capacitive reactance connected to a series resonant circuit. The oscillation frequency $f_{\rm osc}$ is set by the resonant frequency of this circuit according to

$$\frac{1}{j\omega_{\rm osc}C_{\rm act}} + j\omega_{\rm osc}L_{\rm res} + \frac{1}{j\omega_{\rm osc}C_{\rm res}} = 0, \qquad f_{\rm osc} = \frac{\omega_{\rm osc}}{2\pi}. \tag{1}$$

The condition for oscillation is that the negative differential input resistance at least compensates the resonator losses at the oscillation frequency

$$R_{\rm act} + R_{\rm res} < 0 \text{ at } f_{\rm osc}. \tag{2}$$

At start-up of oscillation, the negative resistance of the active device must exceed the resonator losses by about 20% [7]. When steady-state oscillation has built up, large-signal effects cause an increase of the negative resistance and the active device exactly compensates the resonator losses, $R_{\rm act} + R_{\rm res} = 0$.

B. Colpitts Oscillator

The circuit diagram of the 98-GHz VCO is shown in Fig. 2. It is based on the common-collector Colpitts oscillator. In [5] and [8], methods for design and optimization of integrated *LC* oscillators are presented. In [9], a novel method to investigate the phase noise of oscillator is explained. In this paper, the main objective is to evaluate the maximum oscillation frequency of this circuit by means of the negative impedance model.

With the assumption of an ideal transistor Q_1, the impedance of the active device $Z_{\rm act}$ in Fig. 2 can be calculated as

$$Z_{\rm act} = -\frac{g_m}{\omega^2 C_1 C_2} + \frac{1}{j\omega C_1} + \frac{1}{j\omega C_2}. \tag{3}$$

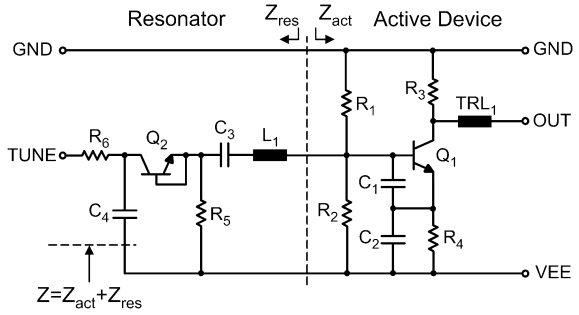

Fig. 2. Circuit diagram of the 98-GHz VCO.

Parasitic elements of transistor Q_1 like the base resistance R_B and the collector-base capacitance C_{BC} increase the real part of $Z_{\rm act}$ and therefore reduce the maximum oscillation frequency. Additionally, the load of transistor Q_1 increases the negative differential resistance of (3). In order to minimize the reduction of the maximum frequency due to the load of Q_1 the grounded coplanar transmission line $\rm TRL_1$ transforms the impedance of the output network, comprising the pad capacitance and the 50-Ω impedance of the measurement equipment in parallel, into a low impedance at the collector of Q_1. This transformation decreases the negative resistance $\rm Re(Z_{act})$ of the oscillator impedance, which enables higher operation frequencies. In Fig. 3, the real and imaginary parts of the simulated impedance $Z = Z_{\rm act} + Z_{\rm res}$ with and without the transmission line $\rm TRL_1$ are shown. The maximum possible oscillation frequency is set by the zero-crossing of $\rm Re(Z)$; see (2). In Fig. 3, it can be seen that oscillation with this configuration is only possible due to the use of transmission line $\rm TRL_1$. The actual oscillation frequency is set by the zero-crossing of the imaginary part $\rm Im(Z)$; see (1).

Large-signal conditions change the voltage-dependent parameters of the transistor. Therefore the results of the linear approach are used as first design results which have to be further optimized by large signal analysis.

C. Resonator

The resonator consists of an inductor L_1, a capacitor C_3 and a diode-connected transistor Q_2. The collector-base capacitance of Q_2 is used as varactor in order to tune the oscillator's frequency. C_4 provides an RF ground at the transistor Q_2. C_1 and C_2 constitute the capacitive voltage divider of the Colpitts oscillator. All capacitors are realized as parallel plate capacitors using metallization layers. The inductance L_1 was designed using a field simulator. A careful optimization of the resonator and the capacitors C_1 and C_2 is necessary in order to increase the quality factor of the resonator and so improve output power and phase noise performance without reducing the maximum oscillation frequency. If the capacitors C_1 and C_2 are large, parasitics of the transistor Q_2 will have a negligible effect but the maximum oscillation frequency will be reduced. A high inductance of L_1 results in a better phase noise but also reduces the maximum oscillation frequency. If the capacitor C_3 in the resonator is small, L_1 could be high at a constant resonant frequency, but the tuning range will be narrowed. C_4 should be as large as possible in order to provide an RF ground at the resonator. As an adequate dimensioning of the components we obtained $C_1 = 17$ fF, $C_2 = 20$ fF, $C_3 = 160$ fF, $C_4 = 710$ fF and $L_1 = 130$ pH. The collector-base capacitance of Q_2 can be set from 150 to 270 fF depending on the tuning voltage. The losses of Q_2 and L_1 are modeled as series resistors with values of 1.7 Ω and 1.4 Ω, respectively.

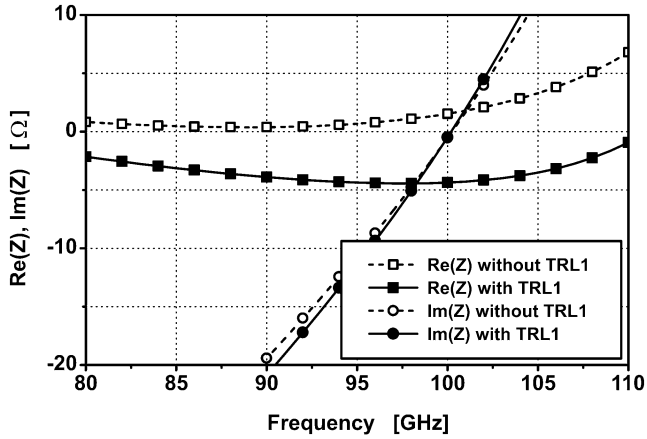

Fig. 3. Simulated impedance $Z = Z_{\rm act} + Z_{\rm res}$ of the 98-GHz VCO.

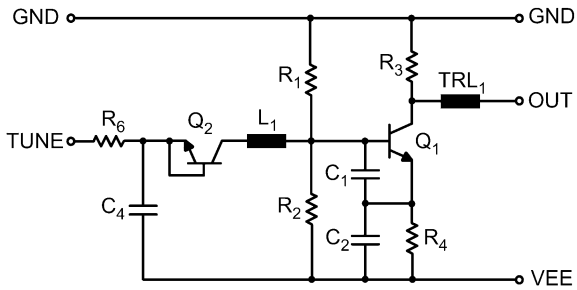

Fig. 4. Circuit diagram of the 84-GHz VCO.

D. 84-GHz VCO

The circuit diagram of the 84-GHz VCO is shown in Fig. 4. In the resonator, the resistor R_5 and the capacitor C_3 are not implemented, as compared to Fig. 2. The polarity of the transistor Q_2 is reversed. These modifications lead to an inverse tuning behavior and a larger tuning range at a slightly lower oscillation frequency.

III. Technology

In this section, the SiGe technology in which the oscillators are fabricated is described [10], [11]. The transistors have a double-polysilicon self-aligned emitter-base configuration with an effective emitter width of 0.18 μm. The SiGe:C base of the transistors has been integrated by selective epitaxial growth. A TEM cross section of the emitter-base configuration is shown in Fig. 5. As seen from this micrograph, the transistor exhibits a monocrystalline emitter contact in the active transistor region without any interfacial native oxide. The emitter resistance of these transistors is reduced by 35% compared to polysilicon emitter devices.

The transistors manufactured in this technology offer a transit frequency f_T of 206 GHz, a maximum oscillation frequency $f_{\rm max}$ of 197 GHz and a ring-oscillator gate delay of 3.9 ps. In Fig. 6, the cut-off frequency f_T versus collector current is shown for three different collector-base voltages.

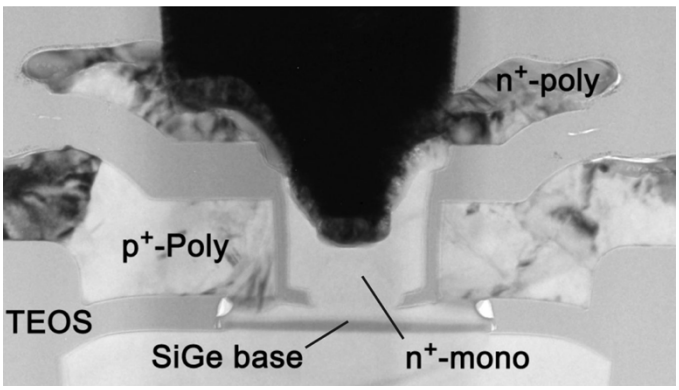

Fig. 5. TEM cross section of the emitter-base complex of a transistor with effective emitter width of 0.18 μm.

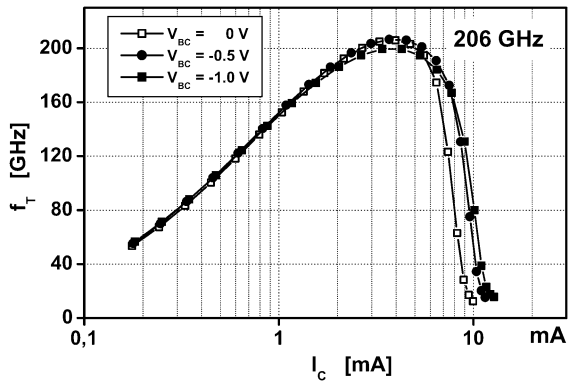

Fig. 6. Cut-off frequency f_T versus collector current I_C of a transistor with an effective emitter size of $0.18 \times 2.8\ \mu\text{m}^2$.

In Table I, the most important transistor parameters of a device with an effective emitter size of $0.18 \times 2.8\ \mu\text{m}^2$ are shown. The technology provides four metallization layers and three different types of polysilicon resistors.

IV. Experimental Results

In Fig. 7, the chip photograph of the 98-GHz VCO is shown. The oscillator core, the metal-metal capacitors, and the transmission lines can be seen clearly. The chip size is 550 μm $\times$ 450 μm.

A. Tuning Characteristic and Output Power

The measurements have been performed on-wafer with an Agilent 8565EC spectrum analyzer, an Agilent 11 970 W harmonic mixer (75–110 GHz), a GGB 120-GHz GSG microwave probe, and a Millitech full-band isolator connected with straight waveguide sections. Due to the losses in the microwave probe and the isolator, there is an attenuation of at least 3 dB in the considered frequency band.

The oscillators operate with a supply voltage of -5 V. This leads to a total current consumption of 12 mA and an emitter current density of 6 mA/μm^2. In Figs. 8 and 9, the measured oscillation frequency and the output power versus the VCO tuning voltage are plotted for the 84-GHz VCO and the 98-GHz VCO, respectively. The measured output power is about -9 dBm, however, due to the losses in the measurement setup, the actual output power is approximately -6 dBm. The frequency steps in the tuning behavior in Figs. 8 and 9 result from influence due to the measurement setup, which is analyzed in Section IV-C.

In Figs. 10 and 11, the measured output spectrum of the VCOs are shown.

TABLE I
Device Parameters

A_E	0.18 x 2.8 μm^2
β	450
R_{BI}	3.0 k$\Omega/\square$
BV_{EBO}	1.8 V
BV_{CEO}	1.8 V
BV_{CBO}	5.8 V
C_{EB}	7.6 fF
C_{BC}	5.7 fF
C_{CS}	6.6 fF
R_B	65 Ω
R_E	4 Ω
R_C	10 Ω
f_T	206 GHz
f_{max}	197 GHz

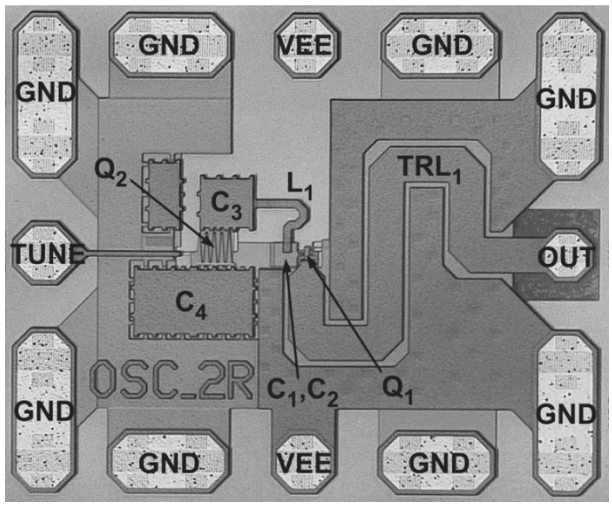

Fig. 7. Chip photograph of the 98-GHz VCO (chip size: 550 μm$\times$ 450 μm).

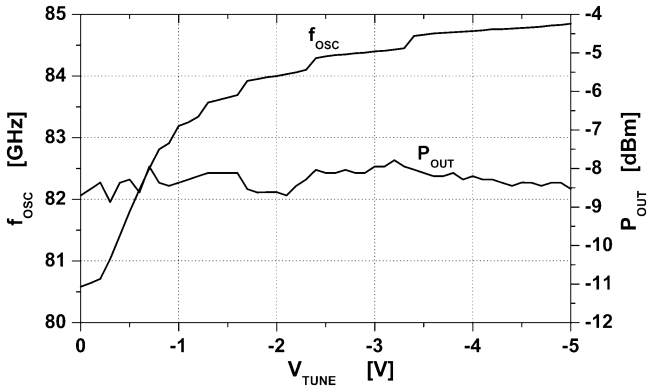

Fig. 8. Measured oscillation frequency and output power versus tuning voltage of the 84-GHz VCO.

B. Phase Noise Measurements

The phase noise performance has been measured with the phase noise measurement system Europtest PN-9000, an Agilent 11 970 W harmonic mixer (75–110 GHz), on-wafer probes

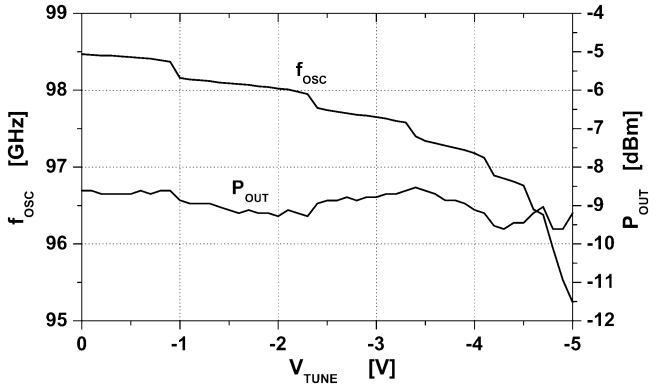

Fig. 9. Measured oscillation frequency and output power versus tuning voltage of the 98-GHz VCO.

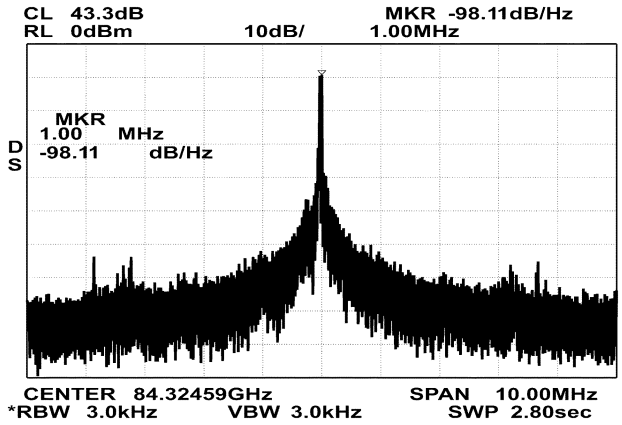

Fig. 10. Measured output spectrum of the 84-GHz VCO.

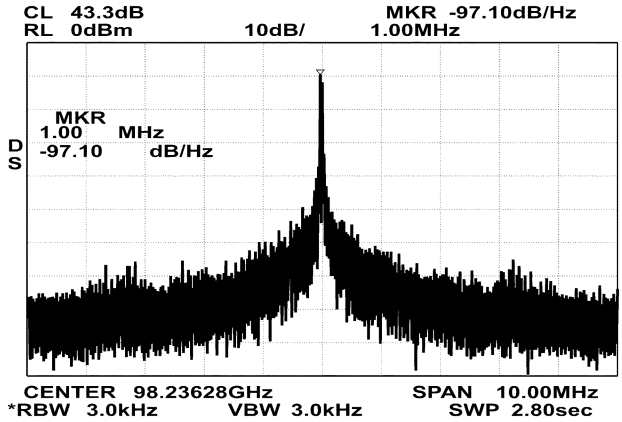

Fig. 11. Measured output spectrum of the 98-GHz VCO.

specified up to 67 GHz, and an Agilent coaxial-to-waveguide adapter V281A. The coaxial system specified only up to 67 GHz in front of the harmonic mixer exhibits about 20 dB loss at 95 GHz. Due to the high loss, matching is improved and the influence of the measurement equipment is avoided. In Fig. 12, the single-sideband phase noise of the 98-GHz VCO versus offset frequency is shown. At an offset frequency of 1 MHz, the phase noise of the 98-GHz VCO is −85 dBc/Hz, the 84-GHz VCO shows −87 dBc/Hz, which fits quite well with simulations. As

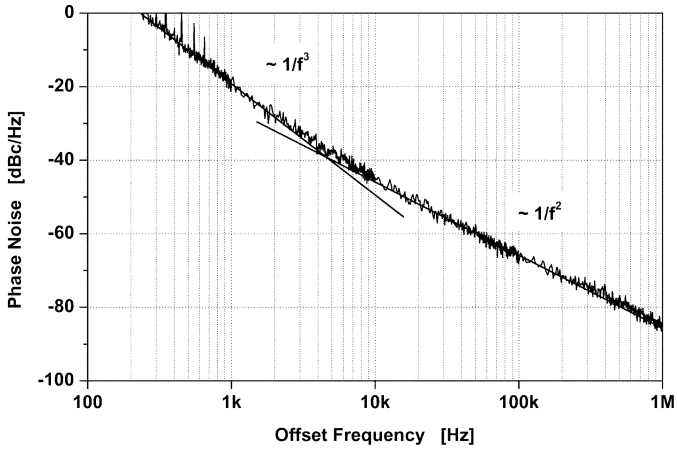

Fig. 12. Measured phase noise of the 98-GHz VCO.

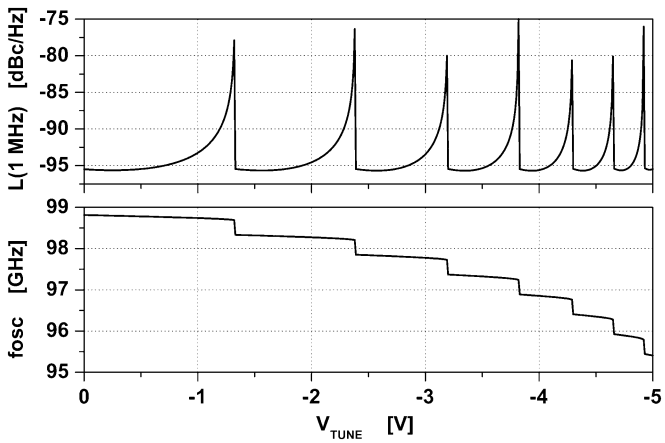

Fig. 13. Simulated tuning behavior and phase noise at 1-MHz offset frequency of the 98-GHz VCO versus a continuously decreasing tuning voltage including the waveguide at the output.

TABLE II
COMPARISON OF STATE-OF-THE-ART OSCILLATORS AND VCOS

Ref.	measured frequency range [GHz]	measured output power [dBm]	measured SSB noise 1 MHz [dBc/Hz]	Technology
[1]	147.6	-18.4	-65	GaAs HBT
[2]	76.1	-7	-91	SiGe:C BiCMOS
[2]	58.7 - 68.5	-17	-84	SiGe:C BiCMOS
[3]	75.3 - 79.6	+14	-94	SiGe HBT
[4]	103.9	-65 [a]	-94 [b]	90 nm CMOS
[5]	36 - 46.9	+9	-110	SiGe HBT
[12]	50.9 - 51.6	-30	-85	120 nm CMOS
[13]	75.3 - 77.8	+7.8	-75	GaAs HEMT
[14]	40.8 - 45.9	—	-96	SiGe BiCMOS
[15]	94.5 - 95.0	-3.5	—	InP HBT
[16]	86 - 94	+7.8	-67	GaAs HFET
this work	95.2 - 98.4	-6	-85	SiGe HBT

[a] including 35 dB conversion loss
[b] at 10 MHz offset frequency

expected, at low offset frequencies the phase noise correspondes to $1/f^3$, and at offset frequencies above 5 kHz, the correspondence is $1/f^2$.

TABLE III
SUMMARY OF TECHNICAL DATA

	84 GHz VCO	98 GHz VCO
Technology	0.18 μm / 206 GHz f_T SiGe bipolar	
Supply voltage	-5.0 V	-5.0 V
Supply current	11.3 mA	12.2 mA
Frequency range	80.5 to 84.8 GHz	95.2 to 98.4 GHz
Measured output power	-8.7 to -7.7 dBm	-9.6 to -8.6 dBm
Phase noise at 1 MHz offset	-87 dBc/Hz (at 84.3 GHz)	-85 dBc/Hz (at 98.2 GHz)
Chip size	550 μm $\times$ 450 μm	550 μm $\times$ 450 μm

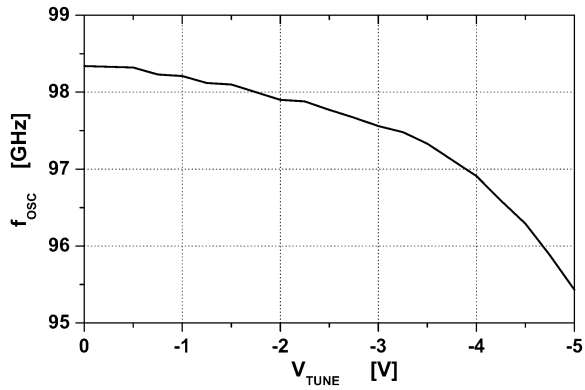

Fig. 14. Oscillation frequency versus tuning voltage of the 98-GHz VCO measured with the coaxial measurement equipment.

C. Influence of Measurement Equipment

The influence of the waveguide components becomes obvious in the frequency steps of the tuning behavior; see Figs. 10 and 11. The height of these steps directly corresponds to the length of the waveguide, which acts as an additional resonator for the oscillator. This resonator not only influences the tuning characteristic, but also improves the phase noise. In Fig. 13, the phase noise of the VCO at 1-MHz offset frequency is simulated versus tuning voltage. In this simulation the waveguide at the output is included. The characteristic in this simulation shows a hysteresis, so in Fig. 13 the tuning voltage was decreased continuously from 0 V to -5 V. The simulated tuning behavior is almost the same as in the measurements; see Fig. 9. It can be seen that the phase noise is subject to strong variations which correspond to the frequency steps. This behavior has been verified by measurements which exhibit a minimum phase noise of -97 dBc/Hz and a maximum phase noise of -85 dBc/Hz, both at 1-MHz offset.

In order to prevent the influence of the waveguide an on-chip output buffer could be used. In the measurements of Fig. 12, the resonator was avoided by applying high losses; see Section IV-B. This measurement setup enabled smooth tuning curves (Fig. 14) and accurate phase noise data at the cost of reduced output power.

V. CONCLUSION

In this paper, a 84-GHz and a 98-GHz VCO implemented in a SiGe bipolar technology have been presented. In Table II, published fundamental-mode, state-of-the-art, fully integrated oscillators and VCOs are compared. Table III summarizes the technical data of the VCOs presented in this work.

ACKNOWLEDGMENT

The authors would like to thank the entire Infineon team which is responsible for fabrication of the chips. The authors are also grateful to H. Tischer for providing measurement equipment and for his support during measurements.

REFERENCES

[1] K. Uchida, H. Matsuura, T. Yakihara, S. Kobayashi, S. Oka, T. Fujita, and A. Miura, "A series of InGaP/InGaAs HBT oscillators up to D-band," *IEEE Trans. Microwave Theory Tech.*, vol. 49, pp. 858–865, May 2001.

[2] W. Winkler, J. Borngräber, B. Heinemann, and P. Weger, "60 GHz and 76 GHz oscillators in 0.25 μm SiGe: C BiCMOS," in *IEEE Int. Solid-State Circuits Conf. (ISSCC) Dig. Tech. Papers*, Feb. 2003, pp. 454–455.

[3] H. Li, H.-M. Rein, and M. Schwerd, "SiGe VCO's operating up to 88 GHz, suitable for automotive radar sensors," *Electron. Lett.*, vol. 39, no. 18, pp. 1326–1327, Sept. 2003.

[4] L. M. Franca-Neto, R. E. Bishop, and B. B. A, "64 GHz and 100 GHz VCO's in 90 nm CMOS using optimum pumping method," in *IEEE Int. Solid-State Circuits Conf. (ISSCC) Dig. Tech. Papers*, 2004, pp. 444–445.

[5] H. Li and H.-M. Rein, "Millimeter-wave VCO's with wide tuning range and low phase noise, fully integrated in a SiGe bipolar production technology," *IEEE J. Solid-State Circuits*, vol. 38, pp. 184–191, Feb. 2003.

[6] W. Perndl, H. Knapp, K. Aufinger, T. F. Meister, W. Simbürger, and A. L. Scholtz, "A 98 GHz voltage controlled oscillator in SiGe bipolar technology," in *Proc. IEEE Bipolar/BiCMOS Circuits and Technology Meeting (BCTM)*, Toulouse, France, Sept. 2003, pp. 67–69.

[7] G. D. Vendelin, *Design of Amplifiers and Oscillators by the S-Parameter Method*. New York: Wiley, 1982.

[8] D. Ham and A. Hajimiri, "Concepts and methods in optimization of integrated LC VCOs," *IEEE J. Solid-State Circuits*, vol. 36, pp. 896–909, June 2001.

[9] A. Hajimiri and T. H. Lee, "A general theory of phase noise in electrical oscillators," *IEEE J. Solid-State Circuits*, vol. 33, pp. 179–194, Feb. 1998.

[10] J. Böck, H. Schäfer, H. Knapp, D. Zöschg, K. Aufinger, M. Wurzer, S. Boguth, M. Rest, R. Schreiter, R. Stengl, and T. F. Meister, "Sub 5 ps SiGe bipolar technology," in *Int. Electron Devices Meeting (IEDM) Tech. Dig.*, Dec. 2002, pp. 763–766.

[11] T. F. Meister, H. Schäfer, K. Aufinger, R. Stengl, S. Boguth, R. Schreiter, M. Rest, H. Knapp, M. Wurzer, A. Mitchell, T. Böttner, and J. Böck, "SiGe bipolar technology with 3.9 ps gate delay," in *Proc. IEEE Bipolar/BiCMOS Circuits and Technology Meeting (BCTM)*, Toulouse, France, Sept. 2003, pp. 103–106.

[12] M. Tiebout, H.-D. Wohlmuth, and W. Simburger, "A 1 V 51 GHz fully-integrated VCO in 0.12 μm CMOS," in *IEEE Int. Solid-State Circuits Conf. (ISSCC) Dig. Tech. Papers*, 2002, pp. 300–301.

[13] H. J. Siweris, H. Tischer, T. Grave, and W. Kellner, "A monolithic W-band HEMT VCO with feedback topology," in *IEEE MTT-S Int. Microwave Symp. Dig.*, vol. 1, June 1999, pp. 17–20.

[14] D. K. Shaeffer and S. Kudszus, "Performance-optimized microstrip coupled VCO's for 40 GHz and 43 GHz OC-768 optical transmission," *IEEE J. Solid-State Circuits*, vol. 38, pp. 1130–1138, July 2003.

[15] H. Wang, L. Tran, J. Cowles, E. Lin, P. Huang, T. Block, D. Streit, and A. Oki, "Monolithic 77- and 94-GHz InP-based HBT MMIC VCOs," in *Proc. IEEE Radio Frequency Integrated Circuits (RFIC) Symp.*, June 1997, pp. 91–94.

[16] A. Bangert, M. Schlechtweg, M. Lang, W. Haydl, W. Bronner, T. Fink, K. Kohler, and B. Raynor, "W-band MMIC VCO with a large tuning range using a pseudomorphic HFET," in *IEEE MTT-S Int. Microwave Symp. Dig.*, vol. 2, June 1996, pp. 525–528.